Title

STROBOSCOPIC MEASUREMENT OF THE g-FACTORS OF THE 7-ISOMER IN 206Pb AND THE 2l/2+ ISOMER IN 207Bi

Authors

Maier, K.H.
Nakai, K.
Leigh, J.R.
et al.

Publication Date

1971-10-01

Submitted to Nuclear Physics

LBL-243
Preprint

STROBOSCOPIC MEASUREMENT OF THE g-FACTORS OF THE 7^- ISOMER IN ^{206}Pb AND THE $21/2^+$ ISOMER IN ^{207}Bi

K. H. Maier, K. Nakai, J. R. Leigh, R. M. Diamond
And F. S. Stephens

October 1971

AEC Contract No. W-7405-eng-48

DISCLAIMER

NUCLEAR MOMENTS (static) ^{206}Pb 7^-, 2200 keV, ^{207}Bi $21/2^+$, 2101.5 keV; measured μ,Iγ (θ)

STROBOSCOPIC MEASUREMENT OF THE g-FACTORS OF THE 7^- ISOMER IN ^{206}Pb AND THE $21/2^+$ ISOMER IN ^{207}Bi*

K. H. Maier†, K. Nakai††, J. R. Leigh‡, R. M. Diamond, and F. S. Stephens

Lawrence Berkeley Laboratory
University of California
Berkeley, California 94720

October 1971

Abstract

The g-factors of the ^{206}Pb 7^- (2200 keV, $T_{1/2}$ = 123μs) and ^{207}Bi $21/2^+$ (2101.5 keV, $T_{1/2}$ = 182μs) isomers have been measured by the stroboscopic method using the $^{204}Hg(\alpha,2n)^{206}Pb$ and $^{204}Hg(^7Li,4n)^{207}Bi$ reactions to excite them. The results are g (^{206}Pb 7^-) = (-0.0217 ± 0.0004)nm and g (^{207}Bi $21/2^+$) = (+0.325 ± 0.006)nm. The implications of these values on the wavefunctions of the states and on the magnetic polarization of the ^{208}Pb core are discussed.

*Work performed under the auspices of the U. S. Atomic Energy Commission.

†NATO fellow on leave from Hahn-Meitner-Institut, Berlin (present address).

††Present Address: Department of Physics, University of Tokyo.

‡Present Address: Department of Nuclear Physics, The Australian National University, Canberra.

1. Introduction

This is one of three related papers on magnetic moments near ^{208}Pb. Although in general the shell model works especially well in this region, its predictions of magnetic moments even for very pure single-particle states deviate appreciably from the experimental results. A study of these deviations was the main interest of this series; the present paper reports on the g-factor measurements of the 7^- isomer ($T_{1/2}$ = 123μs) at 2.200 MeV in ^{206}Pb and the $21/2^+$ level ($T_{1/2}$ = 182μs) in ^{207}Bi. In ref. [1]) we describe the measurement of the $13/2^+$ level in ^{205}Pb, and in ref. [2]) these results are discussed together with other relevant experimental information in regard to their implications in understanding the deviations from the shell-model values.

The ^{206}Pb 7^- level has mainly the configuration $|p_{1/2}^{-1}, i_{13/2}^{-1}\rangle_{7^-}$, and so measuring its g-factor allows a check on the moment of the $i_{13/2}$ neutron orbit as measured in ref. [1]). Alternatively, we can investigate the purity of the state by comparing its moment with that calculated from the $i_{13/2}$ and $p_{1/2}$ neutrons. The $21/2^+$ isomer in ^{207}Bi is proposed by Bergström *et al.*[3]) to result from coupling a $h_{9/2}$ proton to the ^{206}Pb 7^- level. Since the moment of the $h_{9/2}$ proton is known from the ^{209}Bi ground state, we can find out how compatible these three moments are, and again check on the purity of the wavefunctions or on the validity of calculating the moment of a complex state from those of its constituents. Apart from this, we wanted to explore the feasibility of measuring g-factors for lifetimes of the order of 100μs for such heavy nuclei using a liquid metal target, as there are a number of states in this region (with lifetimes up to milliseconds) whose g-factor measurements would be most interesting, and this approach seemed most promising.

2. Experimental Method

The DPAD and SOPAD methods (differential and stroboscopic observation of perturbed angular distributions) following nuclear reactions were used. They can be summarized as follows. (i) A pulsed beam produces an aligned isomeric level through a nuclear reaction. (ii) The conditions for the production are such that the isomer is left in an environment in which the alignment is preserved for a time comparable to the lifetime of the level or longer. (iii) An applied magnetic field causes a Larmor precession of the nuclei which is observed through the corresponding rotation of the angular distribution of the de-exciting γ-rays. At a particular angle this shows up as a modulation of the time distribution of the gamma-ray transitions. The (HI,xnγ) reactions, such as $^{204}Hg(\alpha,2n)^{206}Pb$ and $^{204}Hg(^{7}Li,4n)^{207}Bi$ used here, preferentially populate low-lying high-spin levels due to the large amount of angular momentum brought into the compound nucleus. Since this angular momentum comes almost exclusively from the orbital angular momentum in the entrance channel and so is perpendicular to the beam direction, the isomer will be well aligned. So the first condition regarding cross section and alignment is very favorably fulfilled.

To achieve a relaxation time of the order of 100μs, liquid metal targets seem to be the best choice. Disturbances of the electron shell of the recoiling nucleus and of the surroundings heal very quickly, and the short correlation time of the fluctuating environment tends to average out to zero the fields from neighboring atoms. For the case of the $^{204}Hg(\alpha,2n)^{206}Pb$ 7^- reaction on a liquid mercury target, a time-integral measurement of the g-factor by Quitmann and Jaklevic[4]) had already shown that the relaxation time is at least 100μs. With the choice of the above-mentioned reactions on a liquid mercury target, therefore, the second condition is fulfilled too.

The count rate $I(\Theta,t)$ of a γ-ray de-exciting the isomer at an angle Θ with respect to the beam and at a time t after the centroid of the last beam pulse and with a magnetic field H applied perpendicular to the plane containing the beam and detector is:

$$I(\Theta,t) = \sum_{n=0}^{\infty} \exp(-\lambda(t + nT)) \{1 + A_2 \exp(-\rho(t + nT)) P_2(\cos(\Theta - \omega_L(t + nT))\} \quad . \quad (1)$$

Here $\lambda = 1/\tau$ is the decay constant, T the repetition time of the beam pulses, A_2 the usual coefficient of the angular distribution, $1/\rho = T_r$ the relaxation time, and $\omega_L = -g \cdot H \cdot \mu_N/\hbar$ the Larmor frequency. For the liquid mercury target the relaxation phenomena lead to an exponential decrease of A_2 [5]. The A_4P_4 term of the angular distribution can be neglected, as will become evident.

For $T \gg \tau$, only the first term of the sum has to be considered, and the well-known time-differential method (DPAD) results. By using two detectors simultaneously at angles differing by 90°, the combined count rate

$$\frac{I(\Theta,t) - I(\Theta-90,t)}{I(\Theta,t) + I(\Theta+90,t)} = \frac{3A_2 \exp(-\rho t)\cos(2(\Theta-\omega_L t))}{4 + A_2 \exp(-\rho t)} \quad , \quad (2)$$

can be evaluated. This is essentially a damped sinewave as the denominator varies but little and smoothly. From this the Larmor frequency and relaxation time can easily be extracted.

If, on the contrary $T \ll \tau$, the stroboscopic method results. This has been developed by the group at the Hahn-Meitner-Institut, Berlin [6], and has been discussed in detail in ref. [7] and by Nagamiya and Sugimoto [8]. In this method one counts at an appropriate angle and time window, for instance, $\Theta = 45°$

and $t = 1/4T$, and varies the magnetic field; the count rate will then show a resonance for $\pi/\omega_L = T$, with the area under the resonance determined by A_2 and the width about proportional to $(1/\tau + 1/T_R)$. The setup is shown in fig. 1. To fit the measured data, the sum in eq. (1) has been performed in closed form and so have the integrations over the rectangular beam pulse, the width of the counting window, and the angle covered by the detector. Thus an exact expression was used which is, however, too lengthy to be given here. A considerable improvement in the experiment is achieved with a two detector, two-time-window setup. The double ratio of count rates

$$\frac{I(45°, 1/4T)/I(45°, 3/4T)}{I(-45°, 1/4T)/I(-45°, 3/4T)} \quad , \tag{3}$$

shows the resonance about 4 times stronger, and nearly all errors due to misalignment cancel to first order. Some experimental details are given in the appendix.

3. Results

3.1. ^{206}Pb 7^- STROBOSCOPIC EXPERIMENT

A pulsed beam of 26 MeV α particles from the Berkeley Hilac with T = 20μs repetition time and 4μs pulsewidth was directed on the liquid ^{204}Hg target to excite the isomer. Two planar Ge(Li)-detectors of about 8 cm^3 volume were placed viewing the target at ±45°. The four spectra corresponding to the two detectors and the two time-windows of 4μs width centered at 1/4T and 3/4T were recorded in 2048 channels for each simultaneously (see fig. 1 and appendix for details). The decay scheme of the isomer is shown in fig. 2. Figure 3 gives the observed γ-ray energy spectrum. The branch through the second 4^+ level is too weak to be seen here, but the five lines from the main decay path show up clearly and

can be easily integrated. The stroboscopic resonance curve for the 516 keV line is shown in fig. 4. The solid line is a least-square fit according to eqs. (1) and (3) for g and A_2 with the relaxation time fixed as T_R = 600μs. Similar fits with T_R varying freely have been performed for all 5 transitions and the results are summarized in Table 1. In addition, the fits were repeated with the experimental parameters, such as measuring times and angles, being changed to the maximum possible errors. No significant changes in the answers resulted from this. The only important error in the g-factor determination is that of the magnetic-field measurement which is 1%. The results will be discussed in the next section.

3.2. ^{206}Pb 7^- TIME-DIFFERENTIAL MEASUREMENT

In addition to the stroboscopic experiment, a time-differential measurement was done. The beam was chopped into 10μs wide pulses every 500μs. Using a two-dimensional program on the PDP7 on-line computer, the counts from two detectors at 20° and -70° were recorded as a function of time (512 channels) and energy (4096 channels). The time distribution of the 516 keV line is shown in fig. 5; an averaged background from above and below the line has been subtracted. Figure 6 shows the experimental ratio given by the lefthand side of eq. (2) together with a best fit for g, A_2, T_R according to the righthand side. Actually a phase had to be fitted, too, since the delay between the beam pulse and the start of the measuring interval was only measured with sufficient precision to fix the sign of A_2 and g. For the 803 and 881 keV transitions, only A_2 and T_R were fitted, using g as determined from the 516 keV line. The results are given in Table 1. Again for the g-factor only the 1% error in the

determination of the magnetic field is important. The time calibration was accomplished with quartz-crystal accuracy (see appendix). The asymmetric positioning of the detectors made it possible to determine the sign of A_2 and g unambiguously (the stroboscopic experiment left a common sign undetermined). However, for (HI,xnγ) reactions the sign of A_2 is clearly predicted from the known spins and multipolarities.

As can be seen in Table 1 all results for g show better agreement than the 1% error of the magnetic field. Hence

$$g(^{206}\text{Pb } 7^-) = (-0.0217 \pm 0.0002)\text{nm(uncorrected)} \quad .$$

The actual field at the nucleus can deviate from the applied external magnetic field because of the Knight shift and the diamagnetic correction. The latter is calculated by Feiock and Johnson[9]) as $\Delta H/H = -1.7\%$. The Knight shift for lead dissolved in mercury is unknown. It should, however, be in the range of the measured values of Pb in Pb (1.5%) and Hg in Hg (2.4%[10]). Within the errors this just compensates the diamagnetic shielding, and we, therefore, only increase the error for the corrected g-factor by 1%.

$$g(^{206}\text{Pb } 7^-) = (-0.0217 \pm 0.0004)\text{nm(corrected)} \quad .$$

This can be compared with the result of the previous time-integral measurement[4]) $g = (-0.035 \pm 0.020)$nm. The A_2 coefficients of all three measurements agree rather well and are compatible with about 2/3 of the values calculated for complete alignment of the isomer[11]). This means that the A_4 coefficients are reduced to about 1/4 of the values calculated for complete alignment. Since the latter are smaller than the values of A_2 for complete alignment anyway, the

reduced values of A_4 are negligible, as assumed in the evaluation. The relaxation times as evaluated from the different sets of data scatter widely. Since the lifetime is short compared to the relaxation time the experiment is not very sensitive to this quantity. In addition, the statistics are rather poor. The most likely value for T_R is about 600μs.

3.3. STROBOSCOPIC EXPERIMENT ON ^{207}Bi $21/2^+$

For this isomer only a cursory time-differential measurement was performed to fix the sign of g and to give a starting point in the search for the stroboscopic resonance. The reaction used in this case was ^{204}Hg(^{7}Li,4n)^{207}Bi. The most suitable energy of the ^{7}Li beam was determined from an excitation function to be 41 MeV for the thick target. The setup, including all time intervals, was identical to that of the ^{206}Pb 7^- experiment. The decay scheme of the isomer, as investigated by Bergström et al.[3]), is shown in fig. 7. We have added a 288 keV transition between the two $15/2^-$ levels, since we found a weak line there with about the right halflife. The energy spectrum as seen in the stroboscopic experiment is shown in fig. 8. Unlabeled lines exhibit different half-lives; no attempt was made to assign them. Figure 9 shows the resonance for the 669 keV transition. The 5 strongest lines have been evaluated, and the results are summarized in Table 2. Again the error in the g-factor is determined by the accuracy of the field measurement yielding:

$$g(^{207}\text{Bi } 21/2^+) = (+0.325 \pm 0.0003)\text{nm(uncorrected)} \quad .$$

For correcting the external field to the field at the nucleus, the same situation holds as in the lead case. Therefore:

$$g(^{207}\text{Bi } 21/2^{+}) = (+0.325 \pm 0.006)\text{nm(corrected)} \quad .$$

The spins of the isomer and of the levels populated in its decay have been convincingly proposed by Bergström *et al.*[3]) from a comparison with a shell-model calculation. The A_2 coefficients of the angular distributions established in this measurement are in perfect agreement with this scheme. In addition to the values given in Table 2, the sign of A_2 could be determined for most of the weaker lines; therefore the spins are definite. The relaxation time again is not well determined; the most likely value is $T_R \approx 400\mu s$.

4. Discussion

The principal interest of these measurements was to investigate the deviations of the measured magnetic moments near ^{208}Pb from the predictions of the shell model. This is discussed in a separate article[2]). After a brief examination of the relaxation times, we will discuss here only the information given by the moments about the wavefunctions.

The relaxation times, T_R, of the two isomers in liquid mercury at room temperature have been only roughly determined as 0.5ms in both cases. For the ^{206}Pb 7^- level the relaxation is caused by electric quadrupole interactions. A magnetic interaction is very unlikely due to the small g-factor ($g = -0.0217$), and would require a shorter time by two orders of magnitude for the bismuth isomer since $T_R \sim 1/g^2$. For the $21/2^+$ level in ^{207}Bi with $g = 0.325$, contributions to the relaxation process from magnetic interactions cannot be excluded. However, pure quadrupole relaxation is possible here as well. In this case the quadrupole interaction would have to be about 1.5 times stronger for the bismuth isomer than for the ^{206}Pb 7^- level in order to compensate for the increase of T_R due to the higher spin, according to the theory of Abragam and Pound[5]). With the long relaxation times that we have found, liquid mercury might become a very useful backing for recoil implantations. The chemical inertness and and high Coulomb barrier of mercury are advantageous for this purpose.

Neutron pick-up measurements on ^{207}Pb, ref. [12]), are, within the usual error of roughly 20%, compatible with a pure $(p_{1/2}^{-1}, i_{13/2}^{-1})_{7^-}$ configuration for the ^{206}Pb 7^- level. So this is the dominant part of the wavefunction. The magnetic moment predicted from the pure shell model for this two-particle state is

$\mu = -1.26$nm which is 8 times the measured value, $\mu = -0.15$nm. This discrepancy could be anticipated, since the measured moment of the $i_{13/2}$ neutron hole is only one-half the Schmidt value. If we combine the measured moments[1,13]) of the $p_{1/2}$ and $i_{13/2}$ neutrons using the expression[14]),

$$\mu = gI = \frac{I}{2}(g_1 + g_2) + (g_1 - g_2)\frac{I_1(I_1 + 1) - I_2(I_2 + 1)}{2(I + 1)} \quad , \qquad (4)$$

the result is -0.39nm, which is not too far from the present measurement. However, from the evidence compiled in ref. [2]) we would expect better agreement. Therefore, the greater part of the remaining difference may very well originate from impurities in the wavefunction of the 7^- level. Admixtures are predicted by the calculations of True[15]), which give the wavefunction as:

$$|^{206}\mathrm{Pb}\ 7^-\rangle = 0.952\ (p_{1/2}, i_{13/2})_{7^-} + 0.250\ (f_{5/2}, i_{13/2})_{7^-}$$

$$- 0.169\ (p_{3/2}, i_{13/2})_{7^-} + \cdots \quad .$$

The major correction to the moment comes from the off-diagonal element $\langle p_{1/2}\ i_{13/2}|\mu|p_{3/2}\ i_{13/2}\rangle$. This can be related through merely geometric factors to the measured[16]) B(M1)-value of the $p_{3/2} \rightarrow p_{1/2}$ transition in ^{207}Pb. For the calculation of the three diagonal elements we used the measured moments of the $p_{1/2}$, $f_{5/2}$, and $i_{13/2}$ neutron orbits and the prediction of the effective operator of ref. [2]) for the $p_{3/2}$ orbit, and combined the single-particle g-factors according to the rules for the shell-model magnetic-moment operator[14]). The result is $\mu = -0.27$nm in better agreement with experiment. By increasing the amplitude of the $(p_{3/2}\ i_{13/2})_{7^-}$ component to -0.4, which still is compatible

with the pick-up experiments, the predicted moment becomes $\mu = -0.2n$ which, within the error of the B(M1)-value used, is in agreement with the measured $\mu = -0.15nm$. We would conclude that the sign of the amplitude of the $(p_{3/2},i_{13/2})_{7^-}$ admixture as calculated by True[15]) is right, while the amplitude might have to be increased somewhat. However, some caution is called for, since here we are dealing with very small magnetic moments, and so other perturbations might not be negligible.

In order to see what the present measurement implies about the moment of the $i_{13/2}$ neutron orbit, we can turn the above process around and use the measured moments of the 7^- level and the $p_{1/2}$ neutron to calculate the moment of the $i_{13/2}$ neutron. If we take $\mu((p_{1/2},i_{13/2})_{7^-})$ as the measured value -0.15 plus the correction from the admixtures in True's wavefunction of -0.12nm, and estimate the error to be equal to the correction, the result is $\mu(\nu i^{-1}_{13/2}) = (-0.91 \pm 0.12)nm$. Fortunately, the result is not very sensitive to the uncertainties in the moment of the pure $(p_{1/2},i_{13/2})_{7^-}$ configuration. This agrees with the measured moment of the $13/2^+$ level in ^{205}Pb ($\mu = -0.975 \pm 0.04nm$)[1]) and justifies our assumption[2]) that this value can be taken as the moment of the $i_{13/2}$ neutron orbit.

The situation for the $21/2^+$ level in ^{207}Bi is clear. Calculating its moment from those measured for the ^{206}Pb 7^- level and the $(\pi h_{9/2})$ ^{209}Bi ground state gives $\mu = 3.39nm$ in perfect agreement with the measured $\mu = (3.41 \pm 0.06)nm$. So the proposed wavefunction[3]) $(^{206}Pb\ 7^-, \pi h_{9/2})_{21/2^+}$ is verified. Simultaneously, this is a remarkable example of the validity of combining the measured moments according to the rules for the single-particle operator[14]) even though the individual moments deviate appreciably from the Schmidt values. This, and similar examples confirming the additivity of magnetic moments near ^{208}Pb, are described in ref. [2]).

Acknowledgments

We want to thank Dr. J. Quebert for his help. One of us (K.H.M.) wants to thank the Deutscher Akademischer Austauschdienst for supplying the fellowship for his stay.

Appendix, Experimental Details

TARGET

The liquid mercury target had to be 4mm in diameter due to the beam size. In order to achieve this with the available 80mg of ^{204}Hg (enriched to 80%) the surface tension of the mercury had to be broken so that a target with the shape of a disk could be made. The following procedure worked well. A piece of copper was chromium-plated except for a 0.4mm-deep hole of 4mm diameter. This hole was filled with nitric acid and then the mercury droplet added. Thus the mercury wets the copper and spreads out on it but not onto the chromium. Afterwards the acid is rinsed off. The mutual solubility of copper and mercury is only a few ppm. The bond between the two metals is strong enough to mount the target vertically. To avoid losses under the beam bombardment in vacuo, it was covered with a thin mylar foil.

MAGNETIC FIELD

The magnetic field was provided by an electromagnet with pole pieces 5cm in diameter and with a 2.5cm gap. It was measured with a rotating-coil gaussmeter or by flipping a coil in the field and integrating the induced current. Both devices were calibrated in a precisely-known field before and after the experiments.

TIMING

The timing for the stroboscopic experiments was derived from a 20 Mc/s quartz-crystal oscillator. Every fourth pulse (fig. 1) triggered the electrostatic beam chopper, giving a cycle time of 20μs. The pulsing of the beam is achieved

by applying rectangular high-voltage pulses to a pair of deflection plates that are located between the injector and pre-stripper tank of the Hilac. The clock pulses following and preceding those which trigger the beam open the two count gates. Thus, apart from the uncritical widths, only one delay had to be adjusted to center the windows at 1/4T and 3/4T. This was accomplished by observing the spectrum with a time-to-height converter. For the time-differential measurement the beam pulse and the start of the time-to-height converter were triggered by a scaled-down pulse from a 5 Mc/s quartz-crystal oscillator. The original oscillator pulses were gated by random pulses to reduce the rate, and then triggered a pulser that was fed into the pre-amplifier of the detector. The pulser line provides 20μs markers with quartz-crystal accuracy that are taken simultaneously with the actual measurement.

References

1) K. H. Maier, J. R. Leigh, and R. M. Diamond, Nucl. Phys., to be published

2) K. H. Maier, K. Nakai, J. R. Leigh, R. Diamond, and F. S. Stephens, Nucl. Phys., to be published

3) I. Bergström, C. J. Herrlander, P. Thieberger, and J. Blomqvist, Phys. Rev. 181 (1969) 1642

4) D. Quitmann and J. Jaklevic, Lawrence Radiation Laboratory Report UCRL-18958 (1969)

5) A. Abragam and R. V. Pound, Phys. Rev. 92 (1953) 943

6) J. Christiansen, H.-E. Mahnke, E. Recknagel, D. Riegel, G. Weyer, and W. Witthuhn, Phys. Rev. Letters 21 (1968) 554

7) J. Christiansen, H.-E. Mahnke, E. Recknagel, D. Riegel, G. Schatz, G. Weyer, and W. Witthuhn, Phys. Rev. C1 (1970) 613

8) S. Nagamiya and K. Sugimoto, Osaka University Report OULNS 69-3, 1969

9) F. D. Feiock and W. R. Johnson, Phys. Rev. Letters 21 (1968) 785

10) L. E. Drain, Met. Rev. 12 (1967) 195

11) T. Yamazaki, Nucl. Data A3 (1967) Nr. 1

12) R. Tickle and J. Bardwick, Phys. Rev. 166 (1968) 1167

13) C. M.Lederer, J. M. Hollander, and I. Perlman, Table of Isotopes (Wiley and Sons, 1967, New York)

14) A. de Shalit and I. Talmi, Nuclear Shell Theory (1963), p. 56 and 449

15) W. W. True, Phys. Rev. 168 (1968) 1388

16) H. V. Klapdor, P. von Brentano, E. Grosse, and K. Haberkant, Nucl. Phys. A152 (1970) 263

Table 1. Results of the g-factor measurements of the 7^- isomer in ^{206}Pb. The values given for A_2, the relaxation time T_R, and the g-factor are the results of best fits as described in the text. The g-factors listed are from the stroboscopic experiment except for the one marked (*) which is from the time differential measurement. For comparison, the results of ref. [4]) are included. Column 6 gives the theoretical A_2 for complete alignment of the isomer[11]).

E_γ keV	Multipolarity	A_2 (strob)	A_2 (tdiff)	A_2 (ref. 4)	$A_2 \times U_2$	T_R (strob) μs	T_R (tdiff) μs	g nm
343	M1	-0.21		-0.20	-0.31	950		-0.02168
516	E3	0.51	0.50	0.40	0.77	580	640	-0.02170 -0.02175 *
538	M1	-0.22		-0.17	-0.31	340		-0.02175
803	E2	0.27	0.24	0.25	0.47	1070	2200	-0.02167
881	E2	0.25	0.26	0.24	0.44	710	520	-0.02175

LBL-243

Table 2. Results of the stroboscopic experiment on the ^{207}Bi $21/2^+$ isomer. The values given for A_2, T_R, and g are the results of best fits to the measured resonance as described in the text.

E_γ keV	Multipolarity	A_2	T_R μs	g nm
262	M1 + E2	-0.34	220	0.3258
456	E3	0.43	410	0.3248
669	M1 + E2	-0.62	620	0.3256
713	M1 + E2	-0.44	660	0.3250
743	E3	0.54	390	0.3254

Figure Captions

Fig. 1. Experimental setup of the stroboscopic experiment. Four energy spectra corresponding to the two detectors and two counting intervals were recorded. The derivation of the time intervals from a quartz clock is indicated, and a qualitative intensity distribution of the γ-rays at resonance is shown. (See also text and appendix).

Fig. 2. Decay scheme of the 7^- isomer in ^{206}Pb according to ref. [13].

Fig. 3. Energy spectrum of the decay of the ^{206}Pb 7^- isomer as seen in the stroboscopic experiment. This spectrum is summed over the two counting times.

Fig. 4. Stroboscopic resonance (double ratio of count rates) for the 516 keV E3-transition in the decay of the ^{206}Pb 7^- isomer. The line is a best fit for g and A_2 assuming a relaxation time of 600μs.

Fig. 5. Time-differential g-factor measurement of the ^{206}Pb 7^- level. Shown is the time distribution of the 516 keV transition.

Fig. 6. Ratio of count rates according to eq. (2) for the 516 keV transition in the time-differential g-factor measurement for the ^{206}Pb 7^- isomer. The curve is a best fit for g, A_2, and the relaxation time.

Fig. 7. Decay scheme of the $21/2^+$ isomer in ^{207}Bi. (Derived from ref. [3]).

Fig. 8. Energy distribution of the γ-rays from the decay of the $21/2^+$ isomer in ^{207}Bi as recorded in the stroboscopic experiment analogous to fig. 3.

Fig. 9. Stroboscopic resonance (double ratio of count rates) for the 669 keV (M1-E2)-transition in the decay of the $21/2^+$ isomer in ^{207}Bi. The curve is a best fit for g and A_2 assuming a relaxation time of 400μs.

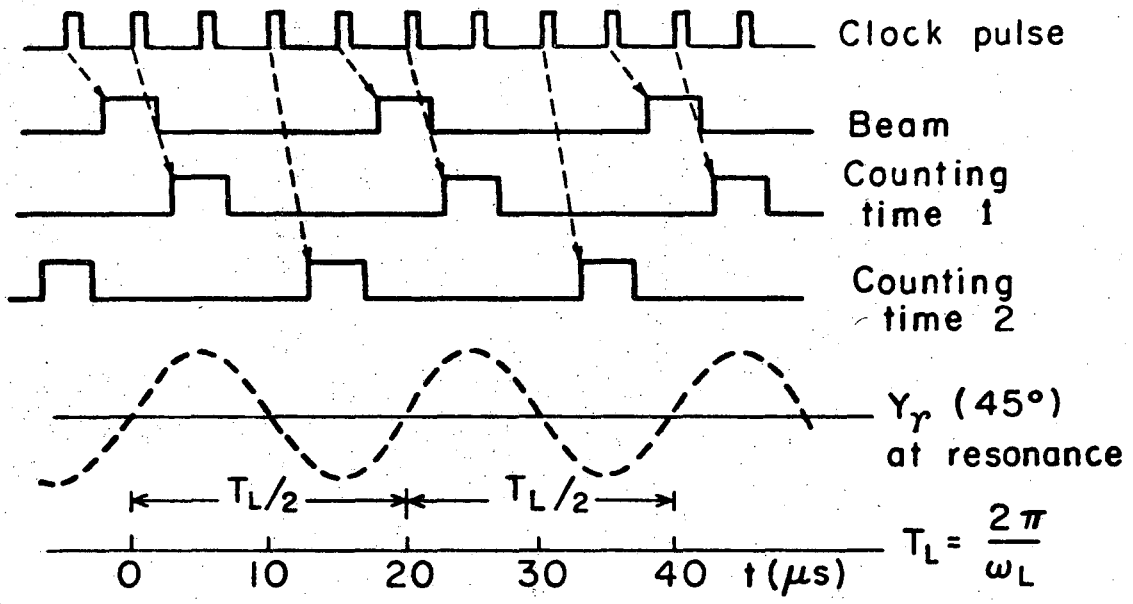

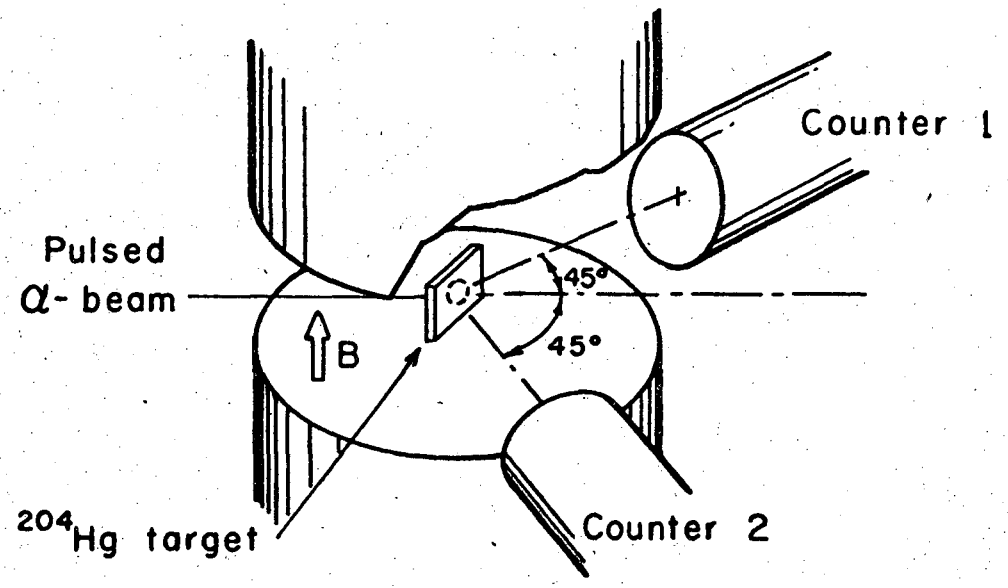

XBL701-2156

Fig. 1

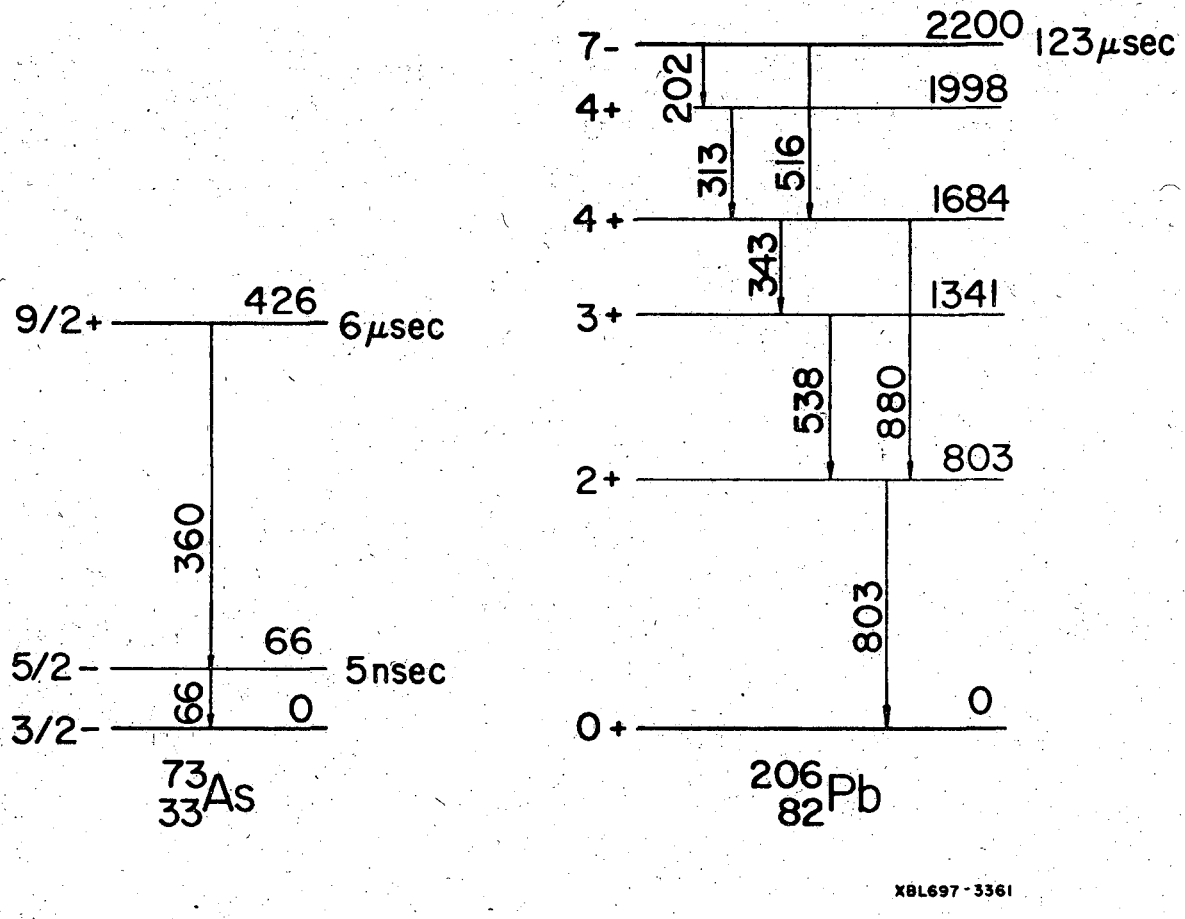
9/2+
426
6μsec
360
66
5nsec
5/2-
66
3/2-
0
73
33As
7-
2200
123μsec
202
4+
1998
313
516
4+
1684
343
3+
1341
538
880
2+
803
803
0+
0
206
82Pb
XBL697-3361

Fig. 2

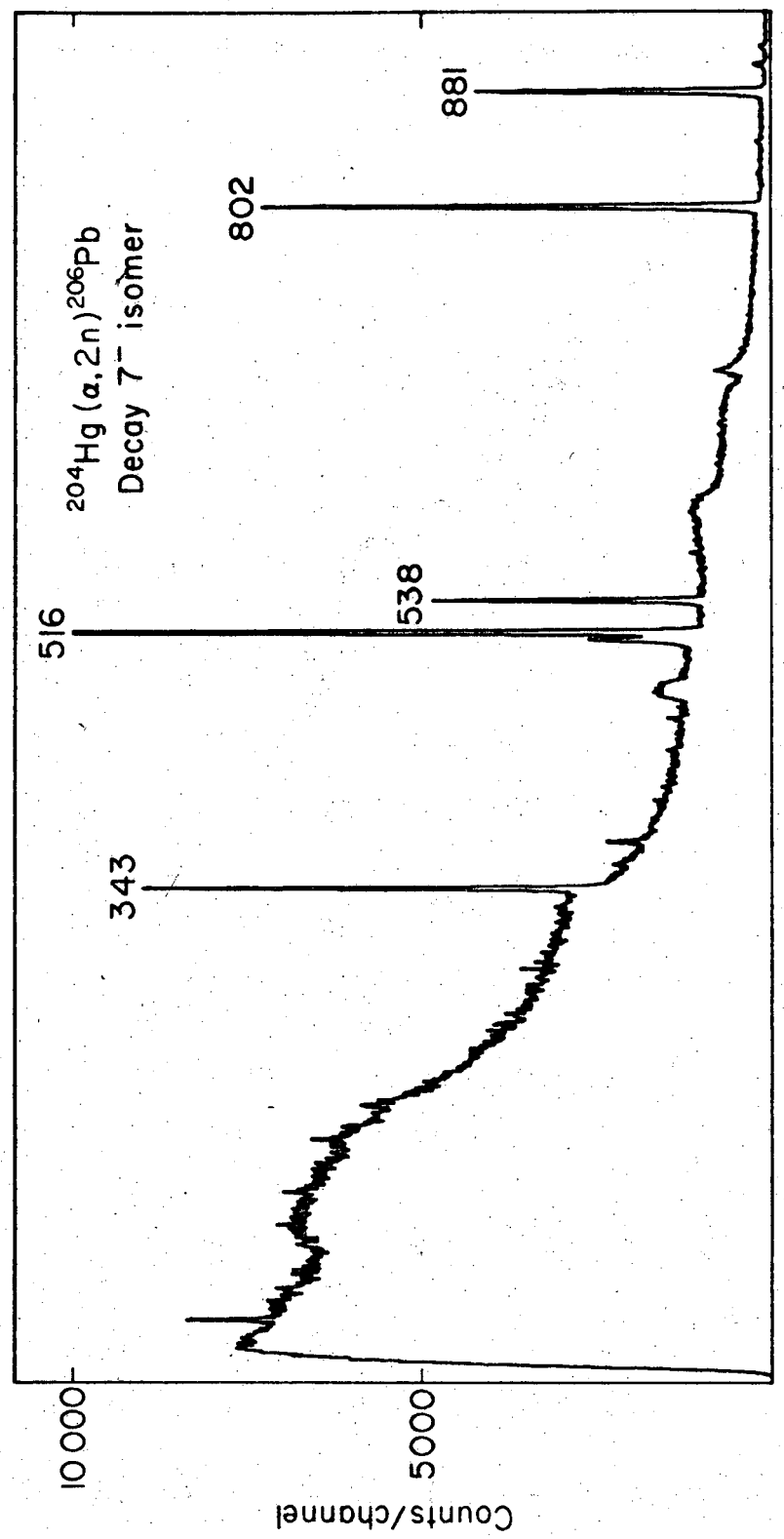

XBL705-2875

Fig. 3

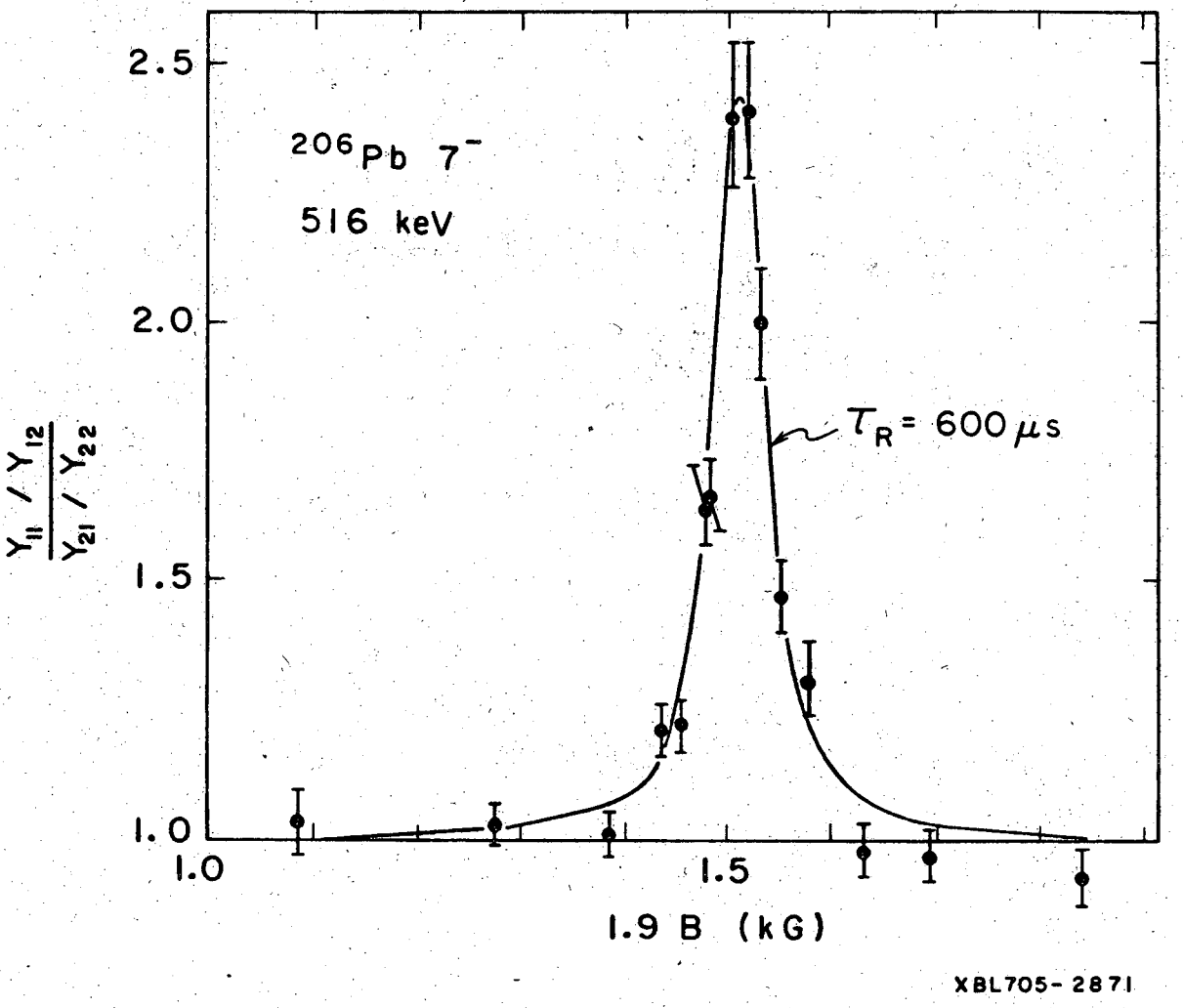
^{206}Pb 7$^-$
516 keV
τ_R = 600 μs
$\frac{Y_{11} / Y_{12}}{Y_{21} / Y_{22}}$
2.5
2.0
1.5
1.0
1.0
1.5
1.9 B (kG)
XBL705-2871

Fig. 4

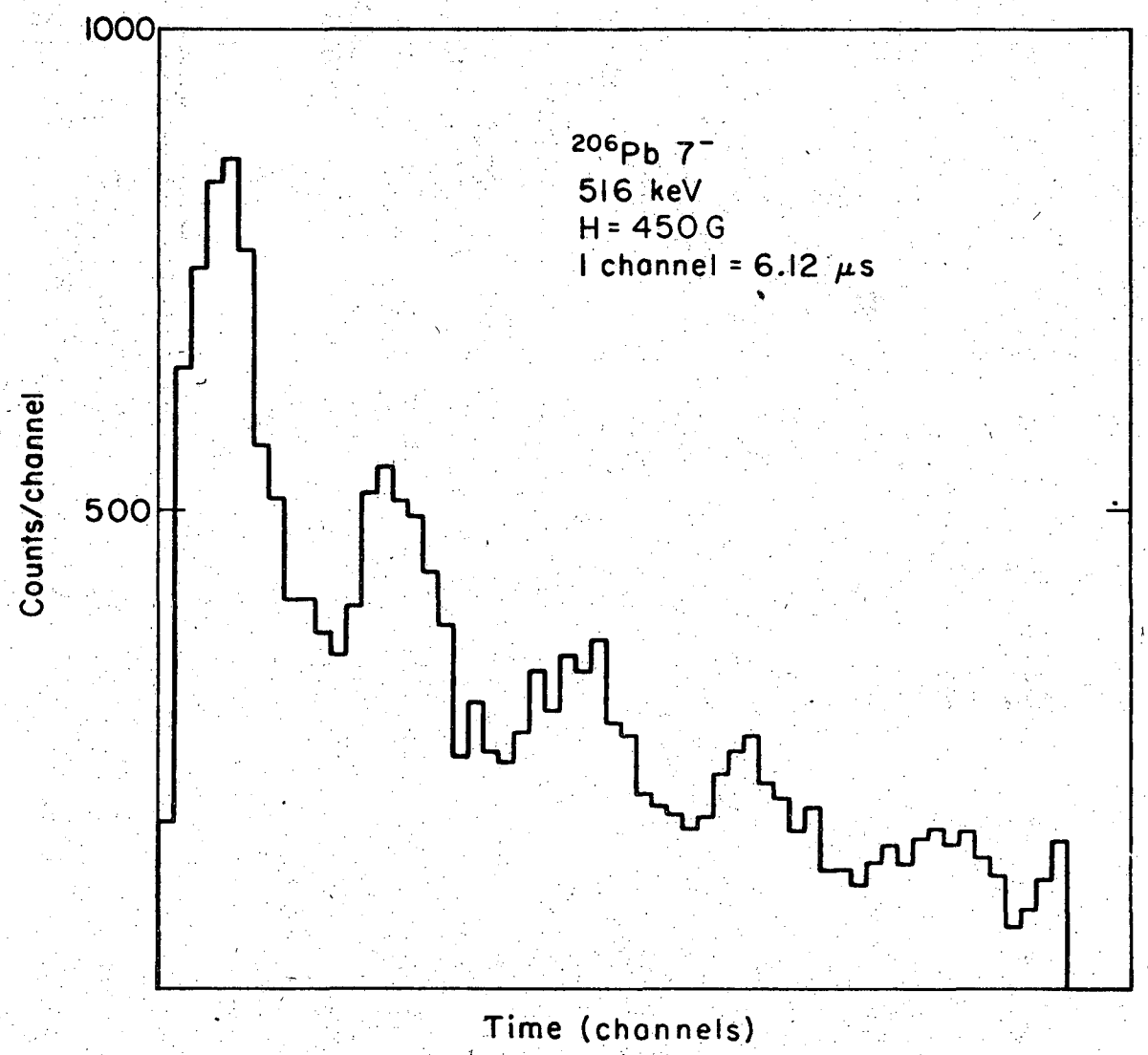

XBL 705-2872

Fig. 5

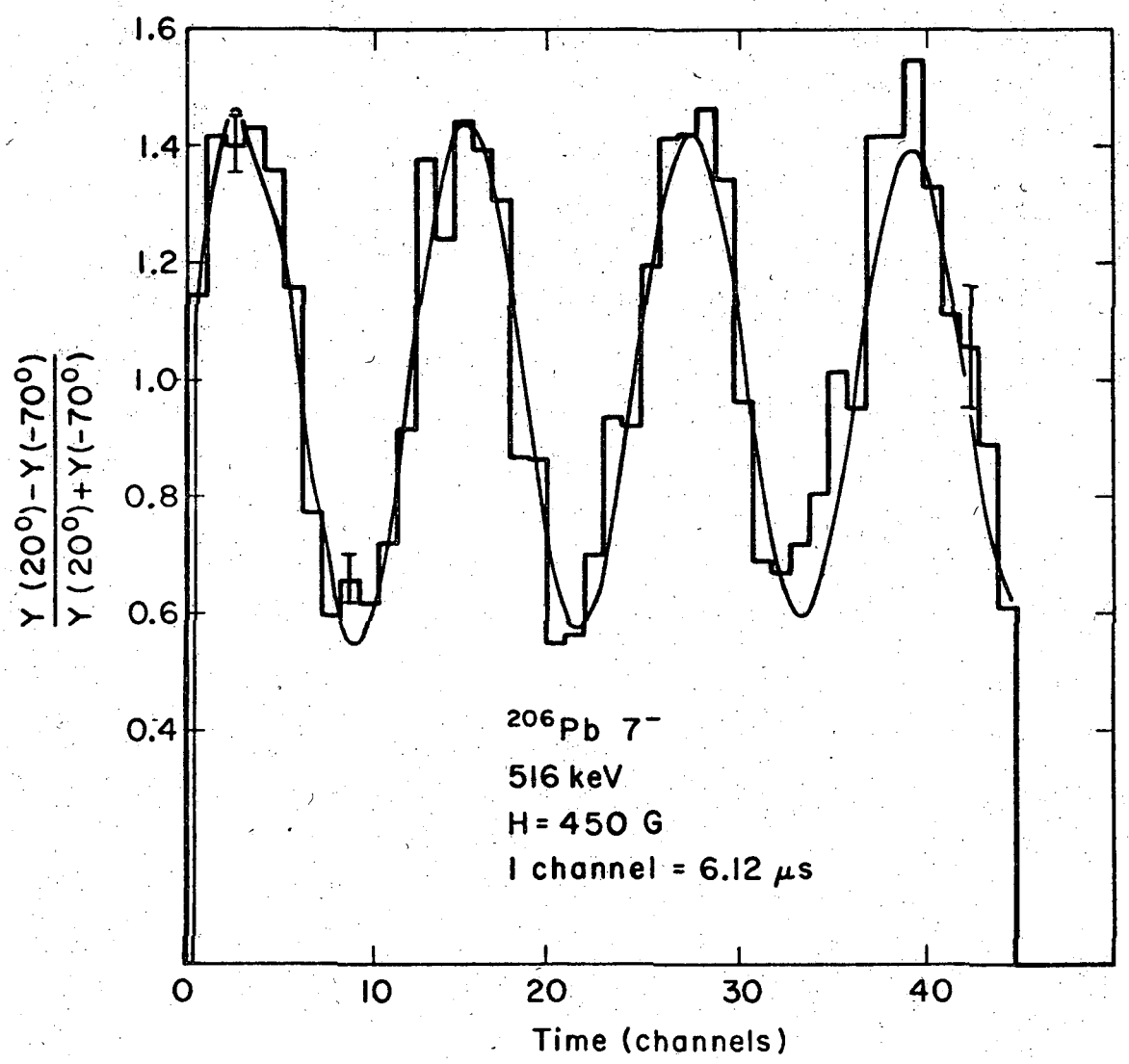

XBL705-2873

Fig. 6

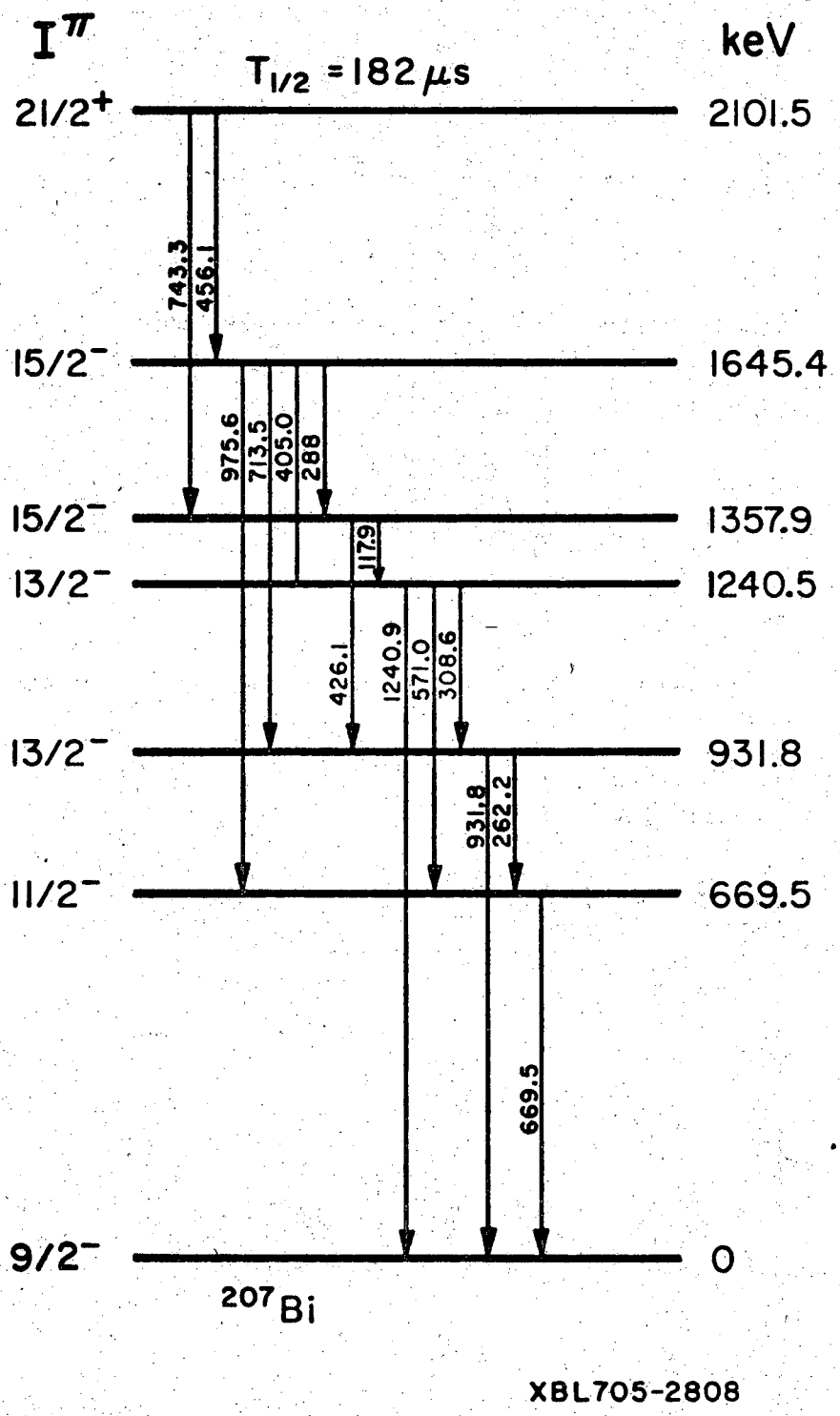

Fig. 7

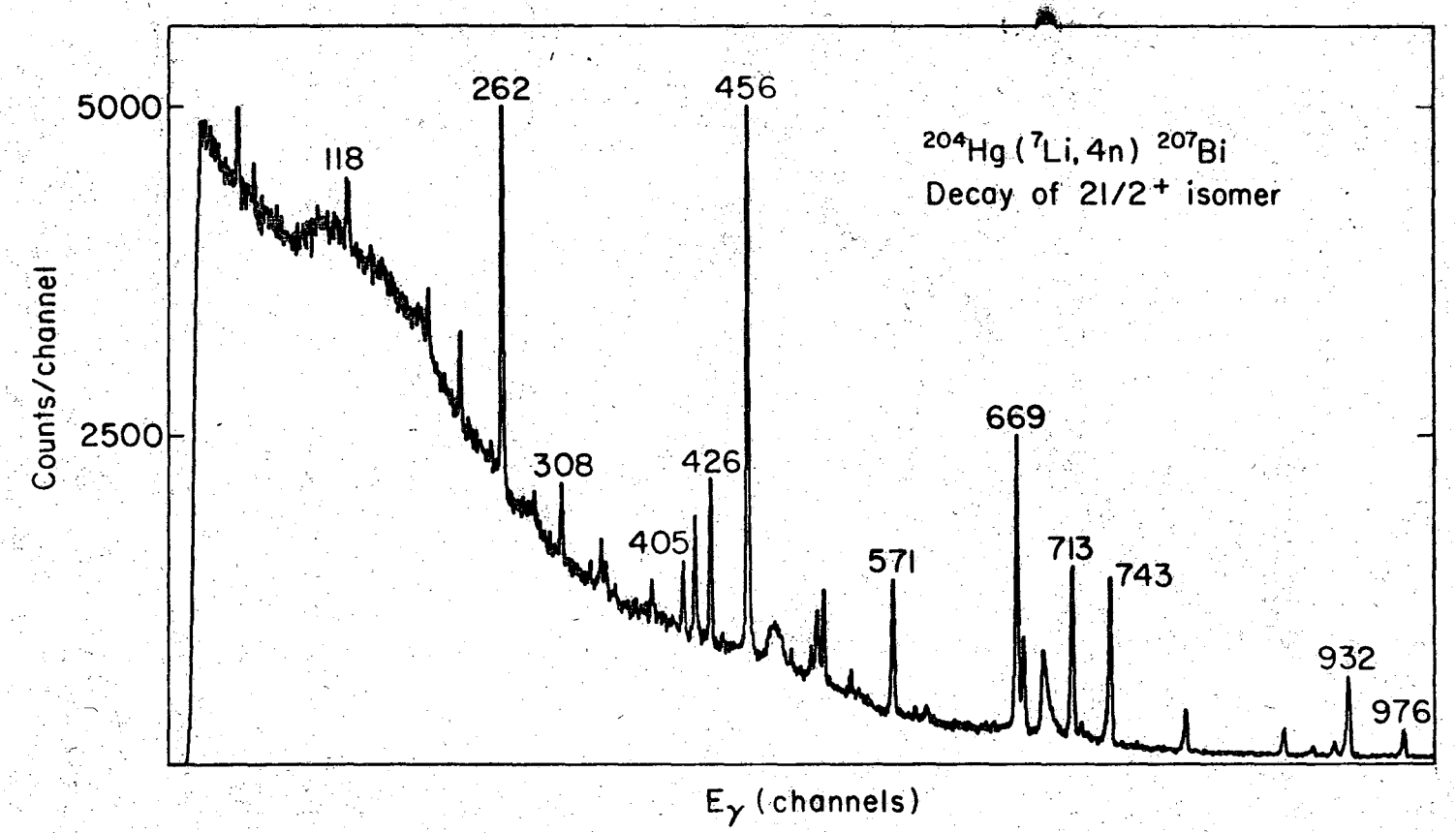

XBL705-2874

Fig. 8

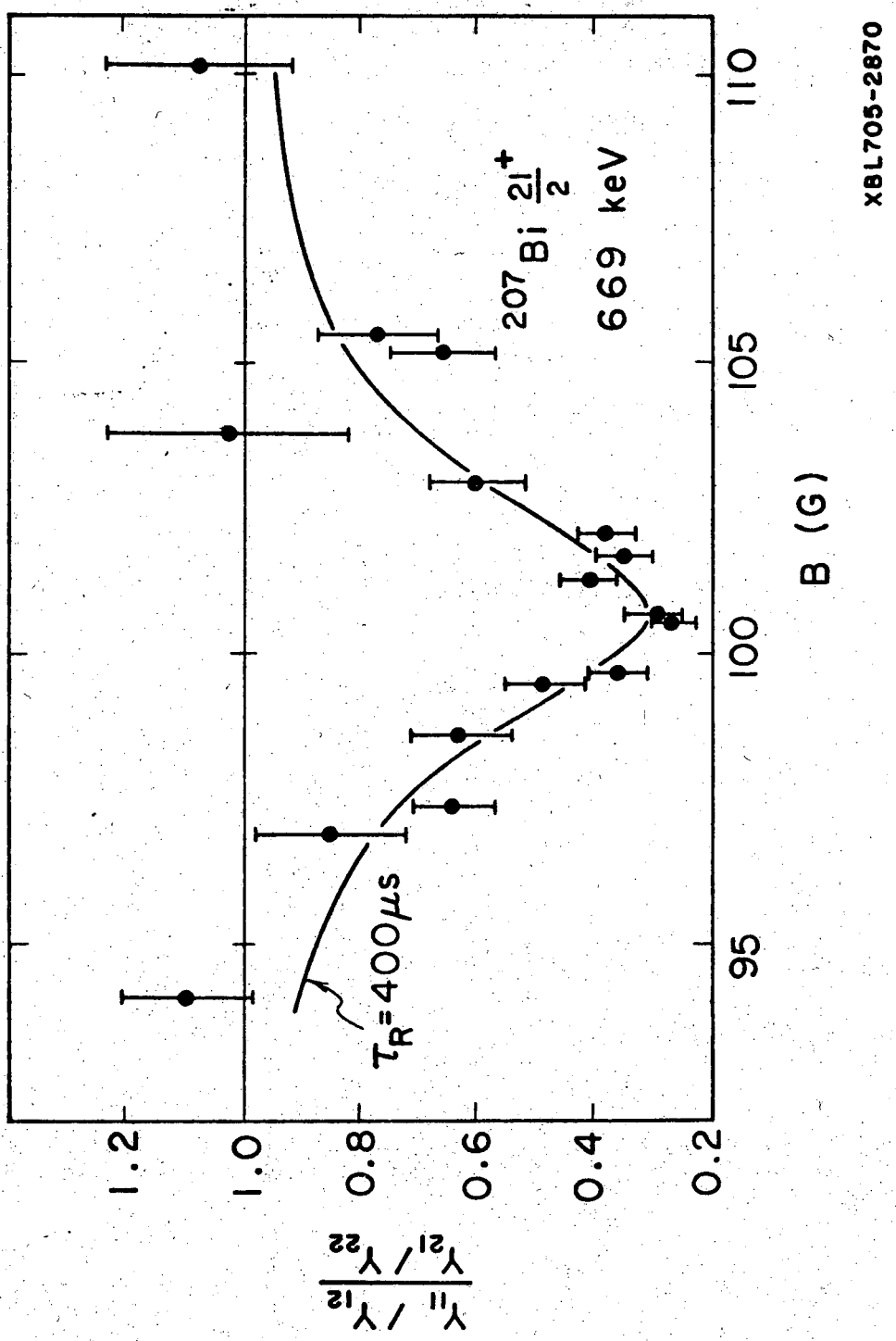
$\frac{\gamma_{11}/\gamma_{12}}{\gamma_{21}/\gamma_{22}}$
1.2
1.0
0.8
0.6
0.4
0.2
95
100
105
110
B (G)
τ_R=400μs
^{207}Bi $\frac{21^+}{2}$
669 keV
XBL705-2870

Fig. 9

TECHNICAL INFORMATION DIVISION
LAWRENCE BERKELEY LABORATORY
UNIVERSITY OF CALIFORNIA
BERKELEY, CALIFORNIA 94720